Journal of Nonlinear Modeling and Analysis
Volume 6, Number 4, December 2024, 998–1021
http://jnma-online.com
DOI:10.12150/jnma.2024.998

Canard Phenomenon and Dynamics for a Slow-Fast Leslie-Gower Prey-Predator Model with Monod-Haldane Function Response

Xiao Wu[1] and Mingkang Ni[2,3,†]

Abstract The geometrical singular perturbation theory has been successfully applied in studying a large range of mathematical biological models with different time scales. In this paper, we use the geometrical singular perturbation theory to investigate a slow-fast Leslie-Gower prey-predator model with Monod-Haldane function response and get some interesting dynamical phenomena such as singular Hopf bifurcation, canard explosion phenomenon,r e laxation oscillation cycle, heteroclinic and homoclinic orbits and the coexis-t e nce of canard cycle and relaxation oscillation cycle.

Keywords Leslie-Gower prey-predator model, slow-fast system, canard explosion phenomenon, relaxation oscillation cycle, heteroclinic orbit, homoclinic orbit

MSC(2010) 34C37, 34C26, 34C07, 37G15.

1. Introduction

Predator-prey model is a typical theme in mathematical biology because of its wide application such as biological invasion of foreign species. In this paper, we mainly investigate the modified Leslie-Gower prey-predator model with Monod-Haldane function response [12, 21, 26] as follows

$$\begin{aligned} \frac{\mathrm{d}u}{\mathrm{d}t} &= u(a_1 - b_1 u) - \frac{c_1 uv}{u^2 + k_1}, \\ \frac{\mathrm{d}v}{\mathrm{d}t} &= v\left(a_2 - \frac{c_2 v}{u^2 + k_2}\right), \end{aligned} \tag{1.1}$$

where u and v separately represent the amount of prey and predators and all parameters are positive and have the following biological meanings: a_1 and a_2 are the natural growth rate of prey and predator which satisfy the assumption that the natural growth rate of prey a_1 is much larger than that of predators a_2; b_1 is the intraspecific competition rate of prey; c_1 measures the reduction of prey due

[†]the corresponding author.
Email address: XiaoWu2022@dhu.edu.cn(X. Wu), xiaovikdo@163.com(M. K. Ni)
[1]School of Mathematics and Statistics, Donghua University, Shanghai 200000, P. R. China
[2]School of Mathematical Sciences, East China Normal University, Shanghai 200000, P. R. China
[3]Shanghai Key Laboratory of Pure Mathematics and Mathematical Practice, Shanghai 200000, P. R. China

to predation; c_2 measures the reduction of predator because of the low density of prey; k_1 and k_2 represent the protection provided by the environment of prey and predators. Note that our assumption is reasonable because the lifespan of predators is very long and they may undergo many different generations of prey, such as hares and lynx, squirrels and coyotes.

For simplicity, using the rescaling transformation

$$\begin{aligned} &\bar{t} = a_1 t, \quad \bar{u} = \frac{b_1 u}{a_1}, \quad \bar{v} = \frac{c_1 b_1^2 v}{a_1^3}, \\ &\epsilon = \frac{a_2}{a_1}, \quad \bar{c} = \frac{c_2 a_1}{c_1 a_2}, \quad \bar{k}_1 = \frac{k_1 b_1^2}{a_1^2}, \quad \bar{k}_2 = \frac{k_2 b_1^2}{a_1^2} \end{aligned}$$

and dropping the bar notation, we rewrite system (1.1) as the following non-dimensional system

$$\begin{aligned} \frac{\mathrm{d}u}{\mathrm{d}t} &= u\left[1 - u - \frac{v}{u^2 + k_1}\right], \\ \frac{\mathrm{d}v}{\mathrm{d}t} &= \epsilon v\left(1 - \frac{cv}{u^2 + k_2}\right). \end{aligned} \tag{1.2}$$

Furthermore, with transformations

$$\tilde{t} = \int_0^t \frac{1}{(u^2 + k_1)(u^2 + k_2)} \mathrm{d}s$$

and $t = \tilde{t}$, system (1.2) can be rewritten as the following topological equivalent form

$$\begin{aligned} \frac{\mathrm{d}u}{\mathrm{d}t} &= u(u^2 + k_2)\left[(1 - u)(u^2 + k_1) - v\right] = f(u, v, \eta), \\ \frac{\mathrm{d}v}{\mathrm{d}t} &= \epsilon v(u^2 + k_1)(u^2 + k_2 - cv) = \epsilon g(u, v, \eta), \end{aligned} \tag{1.3}$$

where $\eta = (c, k_1, k_2)$ and $0 < \epsilon \ll 1$ under our assumption $a_2 \ll a_1$

It is clear that system (1.3) is a slow-fast system with one slow state variable v and one fast state variable u. Using the change of time scale $\tau = \epsilon t$, the system (1.3) can be transformed as

$$\begin{aligned} \epsilon\frac{\mathrm{d}u}{\mathrm{d}\tau} &= u(u^2 + k_2)\left[(1 - u)(u^2 + k_1) - v\right] = f(u, v, \eta), \\ \frac{\mathrm{d}v}{\mathrm{d}\tau} &= v(u^2 + k_1)(u^2 + k_2 - cv) = g(u, v, \eta). \end{aligned} \tag{1.4}$$

Compared with t, the time scale τ is the slow time scale. Hence, systems (1.3) and (1.4) are separately called the fast system and the slow system and their dynamics are equivalent if $0 < \epsilon \ll 1$.

Letting $\epsilon \to 0$ in systems (1.3) and (1.4), we get the degenerate system

$$\begin{aligned} 0 &= f(u, v, \eta), \\ \frac{\mathrm{d}v}{\mathrm{d}\tau} &= g(u, v, \eta), \end{aligned}$$

which is defined on the critical manifold $M_0 = \{(u, v) \mid f(u, v, \eta) = 0\}$, and the layer system

$$\frac{\mathrm{d}u}{\mathrm{d}t} = f(u, v, \eta),$$
$$\frac{\mathrm{d}v}{\mathrm{d}t} = 0.$$

Note that the degenerate system and the layer system are two different approximation of the full system (1.3). Thus, for the dynamics of system (1.3), we need to combine the dynamics of the degenerate system and the layer system in a suitable way. This is the basic idea of the geometric singular perturbation theory.

The geometric singular perturbation theory was first introduced by Fenichel [4], which mainly uses the qualitative methods of ordinary differential equations to study the slow-fast system. Moreover, the normally hyperbolic condition plays an important role in it. If a sub-manifold $\tilde{M}_0 \subset M_0$ satisfies the normally hyperbolic condition, which is the real part of the eigenvalues λ of the Jacobian matrix $\frac{\partial f}{\partial u}(u, v, 0)$ in $\tilde{M}_0$ are nonzero, then there is a slow manifold $\tilde{M}_\epsilon$ near $\tilde{M}_0$ and the dynamics of $\tilde{M}_\epsilon$ are similar to that of $\tilde{M}_0$ based on the Finichel theory [4,9]. For points without the normal hyperbolicity, we analyse them by the blow-up method [7, 8], the entry-exit function [16, 22] and so on.

In recent years, the slow-fast biological models have been a hot point in mathematical biology. Many investigators use the geometric singular perturbation theory to study these models and obtain rich dynamics such as singular Hopf bifurcation, canard cycle, relaxation oscillation cycle, canard explosion phenomena, mix-mode oscillation phenomenon and so on. Especially, relaxation oscillation cycle, canard cycle and canard explosion phenomenon are ubiquitous dynamics in the slow-fast biological models. See Ambrosio et al. [1], Liu et al. [15], Shchepakina [18], Wang et al. [24] and so on. Relaxation oscillation cycle is a periodic orbit consisting of slow and fast sections and Shen et al. [20] reveal its biological meaning. Canard cycle is the flow of a periodic orbit for system (1.3) that still moves along the repelling critical manifold when it passes through the canard point. In [11], Li et al. used the canard cycle to explain the reason that disease persists and breaks out in an SIS epidemic model and the conclusions are extended to an SIRS epidemic model by Zhang et al. [25]. Canard explosion phenomenon, which is studied by Atabaigi et al. [2], Li et al. [10], Wang et al. [23] and so on, is a transition process from a small limit cycle generated in the singular Hopf bifurcation to the relaxation oscillation cycle through a family of canard cycles in an exponentially small parameter range.

In this paper, we mainly study the multi-scale dynamics of system (1.3) by some main tools in the geometric singular perturbation theory, such as the Fenichel theory [4, 9], the normal form [7, 8], the exchange lemma [13, 14], the entry-exit function [16, 22] and so on. The existence of canard cycles, relaxation oscillation cycle, heteroclinic and homoclinic orbits are analysed in detail. Especially, under specific parameter conditions, the relaxation oscillation cycle and canard cycle of system (1.3) coexist. We also give some numerical examples to verify our theoretical results.

The present paper is built up as follows. The equilibriums and slow-fast normal form of system (1.3) are presented in Section 2. We analyse multi-scale dynamics of system (1.3) in Section 3, which include heteroclinic orbits, singular Hopf bifurcation, canard cycles, relaxation oscillation cycle and so on. A brief discussion and

biological explanation are given in the last section.

2. Preliminaries

Based on the biological view point, we investigate system (1.3) in the first quadrant. It is clear that system (1.3) has the following positive invariant set

$$\Omega = \{(u, v) \mid 0 \leq u \leq 1, v \geq 0\}.$$

In this section, we mainly investigate the equilibriums, critical manifolds and slow-fast normal form of system (1.3).

2.1. Equilibriums

Clearly, system (1.3) always has the boundary equilibriums $B_0(0,0)$, $B_1(1,0)$ and $B_2(0, \frac{k_2}{c})$. A straight calculation shows that $B_0(0,0)$ is an unstable node and $B_1(1,0)$ is a saddle point. Moreover, $B_2(0, \frac{k_2}{c})$ is a saddle point with $k_2 < ck_1$ and a stable node with $k_2 > ck_1$. Furthermore, by analysis and straight calculations of the equations

$$f(u, v, \eta) = 0, \quad \epsilon g(u, v, \eta) = 0,$$

we can get the following theorem about the positive equilibriums of system (1.3).

Theorem 2.1. *For the positive equilibriums of system* (1.3)*, the following conclusions hold.*

1. *System* (1.3) *has one positive equilibrium* $E_1(u_1^*, v_1^*)$ *if* $\eta = (c, k_1, k_2) \in D_1$*, where*

$$\begin{aligned}
&D_1 = D_1^1 \cup D_1^2 \cup D_1^3 \cup D_1^4,\\
&D_1^1 = \left\{(c, k_1, k_2) \mid 0 < k_1 < \frac{1}{3}, 0 < c \leq 1, k_2 < ck_1\right\},\\
&D_1^2 = \left\{(c, k_1, k_2) \mid \frac{1}{3}\left(1 - \frac{1}{c}\right)^2 < k_1 < \frac{1}{3}, c > 1, k_2 < ck_1\right\},\\
&D_1^3 = \left\{(c, k_1, k_2) \mid k_1 < \frac{1}{3}\left(1 - \frac{1}{c}\right)^2, c > 1, k_2 < \tilde{k}_2^-\right\},\\
&D_1^4 = \left\{(c, k_1, k_2) \mid k_1 < \frac{1}{4}\left(1 - \frac{1}{c}\right)^2, c > 1, k_2 \leq \tilde{k}_2^+\right\},\\
&\tilde{k}_2^+ = c(1 - \tilde{u}_+)(\tilde{u}_+ + k_1) - \tilde{u}_+^2, \quad \tilde{k}_2^- = c(1 - \tilde{u}_-)(\tilde{u}_- + k_1) - \tilde{u}_-^2.
\end{aligned}$$

2. *System* (1.3) *has two positive equilibriums* $E_1(u_1^*, v_1^*)$ *and* $E_2(u_2^*, v_2^*)$ *if* $\eta = (c, k_1, k_2) \in D_2^1 \cup D_2^2 \cup D_2^3$*, where*

$$\begin{aligned}
&D_2^1 = \left\{(c, k_1, k_2) \mid k_1 < \frac{1}{4}\left(1 - \frac{1}{c}\right)^2, c > 1, ck_1 < k_2 < \tilde{k}_2^+\right\},\\
&D_2^2 = \left\{(c, k_1, k_2) \mid k_1 < \frac{1}{3}\left(1 - \frac{1}{c}\right)^2, c > 1, k_2 = \tilde{k}_2^-\right\},
\end{aligned}$$

$$D_2^3 = \left\{ (c, k_1, k_2) \mid \frac{1}{4}\left(1-\frac{1}{c}\right)^2 < k_1 < \frac{1}{3}\left(1-\frac{1}{c}\right)^2, c > 1, k_2 = \tilde{k}_2^+ \right\}.$$

3. System (1.3) *has three positive equilibriums* $E_1(u_1^*, v_1^*)$, $E_2(u_2^*, v_2^*)$ *and* $E_3(u_3^*, v_3^*)$ *if* $\eta = (c, k_1, k_2) \in D_3$, *where*

$$D_3 = \left\{ (c, k_1, k_2) \mid k_1 < \frac{1}{3}\left(1-\frac{1}{c}\right)^2, c > 1, \tilde{k}_2^- < k_2 < \min\left\{ ck_1, \tilde{k}_2^+ \right\} \right\}.$$

2.2. The critical manifold

Let $\epsilon \to 0$ in systems (1.3) and (1.4). We get the degenerate system

$$\begin{aligned} 0 &= u(u^2+k_2)\left[(1-u)(u^2+k_1)-v\right], \\ \frac{\mathrm{d}v}{\mathrm{d}\tau} &= v(u^2+k_1)(u^2+k_2-cv) \end{aligned} \tag{2.1}$$

and the layer system

$$\begin{aligned} \frac{\mathrm{d}u}{\mathrm{d}t} &= u(u^2+k_2)\left[(1-u)(u^2+k_1)-v\right], \\ \frac{\mathrm{d}v}{\mathrm{d}t} &= 0. \end{aligned} \tag{2.2}$$

Hence, some analyses show that the critical manifold is

$$M_0 = M_0^1 \cup M_0^2 = \{(u,v) \mid u = 0\} \cup \left\{(u,v) \mid v = h_1(u) = (1-u)(u^2+k_1)\right\}, \tag{2.3}$$

which has three non-normally hyperbolic points $Q_0(0, k_1)$, $Q_m(u_m, v_m)$ and $Q_M(u_M, v_M)$ with $u_m = \frac{1-\sqrt{1-3k_1}}{3}$ and $u_M = \frac{1+\sqrt{1-3k_1}}{3}$. Moreover, u_m and u_M satisfy $0 < u_m < \frac{1}{3} < u_M < \frac{2}{3}$ if $k_1 < \frac{1}{3}$. Hence, in what follows, we are keen on the dynamics of system (1.3) in the following parameters region

$$D = \left\{ (c, k_1, k_2) \mid 0 < k_1 < \frac{1}{3}, c > 0, k_2 > 0 \right\}.$$

Furthermore, the points $Q_m(u_m, v_m)$ and $Q_M(u_M, v_M)$ split M_0^2 into normally hyperbolic attracting parts

$$\begin{aligned} M_0^{2l} &= \{(u,v) \mid v = h_1(u),\ 0 < u < u_m\}, \\ M_0^{2r} &= \{(u,v) \mid v = h_1(u),\ u_M < u < 1\} \end{aligned}$$

and normally hyperbolic repelling part

$$M_0^{2m} = \{(u,v) \mid v = h_1(u),\ u_m < u < u_M\}.$$

The point $Q_0(0, k_1)$ divides M_0^1 into the normally hyperbolic stable manifold

$$M_0^{1s} = \{(u,v) \mid u = 0,\ v > k_1\}$$

and the normally hyperbolic unstable manifold

$$M_0^{1u} = \{(u,v) \mid u = 0,\ 0 < v < k_1\}.$$

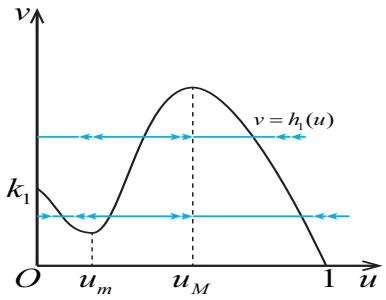

Figure 1. The normal hyperbolic parts of critical manifold M_0.

See Fig.1.

Next, we study the dynamics of system (1.3) near non-normally hyperbolic points $Q_0(0, k_1)$, $Q_m(u_m, v_m)$ and $Q_M(u_M, v_M)$. Clearly, for $\epsilon > 0$, a trajectory starting at point (u_0, v_0) near M_0^{1s} tends quickly toward M_0^{1s} and never crosses it, then drifts downwards along the v-axis at a slow speed $O(\epsilon)$. Finally, this trajectory tends quickly away from M_0^{1u} in the neighborhood of $(0, p_\epsilon(v_0))$ which satisfies $\lim_{\epsilon\to 0} p_\epsilon(y_0) = p_0(y_0)$. The function $p_0(v_0)$ is called the entry-exit function, which is a C^∞ function of (ϵ, y_0) [16, 22]. When $k_2 < ck_1$, the exit-entry function of system (1.3) satisfies the following lemma.

Lemma 2.1. *For system* (1.3)*, if* $k_2 < ck_1$ *and fixed* $v^0 \in (k_1, +\infty)$*, there is a unique* $\hat{v}_* \in (\frac{m_2}{b}, m_1)$ *such that*

$$\int_{v^0}^{\hat{v}_*} \frac{f_1(0, v, \eta)}{g(0, v, \eta)} \mathrm{d}v = 0, \tag{2.4}$$

where $f(u, v, \eta) = u f_1(u, v, \eta)$.

Proof. Let

$$I(\hat{v}) = \int_{v^0}^{\hat{v}} \frac{f_1(0, v, \eta)}{g(0, v, \eta)} \mathrm{d}v = \frac{k_2}{ck_1} \int_{v^0}^{\hat{v}} \frac{v - k_1}{v\left(v - \frac{k_2}{c}\right)} \mathrm{d}v. \tag{2.5}$$

Clearly, we have $\lim_{\hat{v}\to k_2/c} I(\hat{v}) = +\infty$ and $I(k_1) < 0$. Indeed, we also have

$$I'(\hat{v}) = \frac{k_2}{ck_1} \frac{\hat{v} - k_1}{\hat{v}\left(\hat{v} - \frac{k_2}{c}\right)} < 0, \quad \hat{v} \in (\frac{k_2}{c}, k_1).$$

Hence, we can conclude that there is a unique $\hat{v}_* \in (\frac{k_2}{c}, k_1)$ such that $I(\hat{v}_*) = 0$. □

2.3. Slow-fast normal form

In order to analyse the dynamics near the non-normally hyperbolic points (u_m, v_m) and (u_M, v_M), we need to obtain the slow-fast normal form of system (1.3) near (u_m, v_m) and (u_M, v_M) based on the results in [7, 8]. In what follows, we mainly derive the slow-fast normal form near the point (u_m, v_m) and a similar conclusion

is also true for the point (u_M, v_M). To begin with, we transform the fold point (u_m, v_m) into the origin point and obtain

$$\begin{aligned}\frac{\mathrm{d}u}{\mathrm{d}t} &= -p_1 v + u^2\left[p_2 + p_3 u + p_4 u^2 + O\left(|u,v|^3\right)\right],\\ \frac{\mathrm{d}v}{\mathrm{d}t} &= \epsilon\left[q_0 + q_1 u + q_2 u^2 + v\left(r_0 + r_1 u + r_2 v\right) + O\left(|u,v|^3\right)\right],\end{aligned} \tag{2.6}$$

where

$$\begin{aligned}&p_1 = u_m\left(u_m^2 + k_2\right) + O(u), \quad p_2 = u_m\left(u_m^2 + k_2\right)\left(1 - 3u_m\right),\\ &p_3 = u_m^2\left(3 - 10u_m\right) + k_2(1 - 4u_m), \quad p_4 = 3u_m - 12u_m^2 - k_2,\\ &r_0 = \left(u_m^2 + k_1\right)\left(u_m^2 + k_2 - 2cv_m\right),\\ &r_1 = 2u_m\left(2u_m^2 + k_1 + k_2 - 2cv_m\right), \quad r_2 = -c\left(u_m^2 + k_1\right),\\ &q_0 = \left(u_m^2 + k_1\right)v_m\left(u_m^2 + k_2 - cv_m\right), \quad q_1 = 2u_m v_m\left(2u_m^2 + k_1 + k_2 - cv_m\right),\\ &q_2 = v_m\left(6u_m^2 + k_1 + k_2 - cv_m\right).\end{aligned}$$

Note that $p_2 > 0$ and we can choose a suitable value of c such that $q_1 > 0$ and $q_0 < 0$.

Hence, we set

$$\lambda = -\frac{p_2 q_0}{q_1^{\frac{3}{2}} p_1^{\frac{1}{2}}} = -\frac{\left(1 - 3u_m\right)\left(u_m^2 + k_1\right)}{2u_m}\sqrt{\frac{u_m^2 + k_2}{2v_m}}\frac{\left(u_m^2 + k_2 - cv_m\right)}{\left(2u_m^2 + k_1 + k_2 - cv_m\right)^{\frac{3}{2}}} \tag{2.7}$$

and rewrite system (2.6) as the following normal form

$$\begin{aligned}\frac{\mathrm{d}u}{\mathrm{d}t} &= -v h_1(u,v,\lambda) + u^2 h_2(u,v,\lambda) + \epsilon h_3(u,v,\lambda),\\ \frac{\mathrm{d}v}{\mathrm{d}t} &= \epsilon\left(u h_4(u,v,\lambda) - \lambda h_5(u,v,\lambda) + v h_6(u,v,\lambda)\right),\end{aligned} \tag{2.8}$$

where

$$\begin{aligned}&h_1(u,v,\lambda) = 1, \quad h_2(u,v,\lambda) = 1 + \frac{p_3\sqrt{p_1 q_1}}{p_2^2}u + \frac{p_4 p_1 q_1}{p_2^3}u^2 + O\left(|u,v|^3\right),\\ &h_3(u,v,\lambda) = 0, \quad h_4(u,v,\lambda) = 1 + \frac{q_2}{p_2}\sqrt{\frac{p_1}{q_1}}u + O\left(|u,v|^2\right),\\ &h_5(u,v,\lambda) = 1, \quad h_6(u,v,\lambda) = \frac{r_0}{\sqrt{p_1 q_1}} + \frac{r_1}{p_2}u + \frac{r_2}{p_2}\sqrt{\frac{q_1}{p_1}}v + O\left(|u,v|^2\right).\end{aligned}$$

It is clear that $\lambda = 0$ is equal to $q_0 = 0$, which has a solution $c = \left(u_m^2 + k_2\right)v_m^{-1} \triangleq c_m$.

Thus, based on the conclusions of [7, 8], we have

$$\begin{aligned}&a_1 = \frac{\partial h_3}{\partial u}(0,0,0) = 0, \quad a_2 = \frac{\partial h_1}{\partial u}(0,0,0) = 0,\\ &a_3 = \frac{\partial h_2}{\partial u}(0,0,0) = \frac{\sqrt{2v_m\left(u_m^2 + k_1\right)\left(u_m^2 + k_2\right)}\left[u_m^2(3 - 10u_m) + k_2(1 - 4u_m)\right]}{u_m\left(u_m^2 + k_2\right)^2\left(1 - 3u_m\right)^2},\end{aligned}$$

$$a_4 = \frac{\partial h_4}{\partial u}(0,0,0) = \frac{\left(5u_m^2 + k_1\right)}{u_m(1-3u_m)}\sqrt{\frac{v_m}{2\left(u_m^2+k_2\right)\left(u_m^2+k_1\right)}},$$

$$a_5 = h_6(0,0,0) = -\frac{1}{u_m}\sqrt{\frac{\left(u_m^2+k_2\right)\left(u_m^2+k_1\right)}{2v_m}}$$

and

$$\begin{aligned} A &= -a_2 + 3a_3 - 2a_4 - 2a_5 \\ &= \frac{\hat{A}}{u_m\left(u_m^2+k_2\right)^2(1-3u_m)^2}\sqrt{\frac{2\left(u_m^2+k_2\right)\left(u_m^2+k_1\right)}{v_m}}, \end{aligned}$$

where

$$\begin{aligned} \hat{A} &= (1-3u_m)\left(u_m^2+k_2\right)\left[u_m^2+k_2-u_m(u_m^2+2+3k_2)\right] \\ &\quad + 3v_m\left[k_2(1-4u_m)+(3-10u_m)u_m^2\right]. \end{aligned}$$

Furthermore, system (2.8) has the singular Hopf bifurcation curve $\lambda = \lambda_H(\sqrt{\epsilon})$ and the maximal canard curve $\lambda = \lambda_c(\sqrt{\epsilon})$ as

$$\begin{aligned} \lambda_H(\sqrt{\epsilon}) &= -\frac{a_1+a_5}{2}\epsilon + O\left(\epsilon^{\frac{3}{2}}\right) \\ &= \frac{1}{2u_m}\sqrt{\frac{\left(u_m^2+k_2\right)\left(u_m^2+k_1\right)}{2v_m}}\epsilon + O\left(\epsilon^{\frac{3}{2}}\right) \end{aligned} \tag{2.9}$$

and

$$\begin{aligned} \lambda_c(\sqrt{\epsilon}) &= -\left(\frac{a_1+a_5}{2}+\frac{A}{8}\right)\epsilon + O\left(\epsilon^{\frac{3}{2}}\right) \\ &= \frac{1}{2u_m}\sqrt{\frac{\left(u_m^2+k_2\right)\left(u_m^2+k_1\right)}{2v_m}}\left[1-\frac{\hat{A}}{2\left(u_m^2+k_2\right)^2(1-3u_m)^2}\right]\epsilon \\ &\quad + O\left(\epsilon^{\frac{3}{2}}\right). \end{aligned} \tag{2.10}$$

Since

$$\lambda'(c) = \frac{(1-3u_m)\left(u_m^2+k_1\right)}{4u_m}\sqrt{\frac{\left(u_m^2+k_2\right)v_m}{2}}\frac{2k_1-k_2+u_m^2+cv_m}{(k_1+k_2+2u_m^2-cv_m)^{\frac{5}{2}}},$$

we can choose a suitable c such that $\lambda'(c) > 0$ which implies that the function $\lambda(c)$ is increasing as the value of c increases. Thus, the equations $\lambda(c) = \lambda_H(\sqrt{\epsilon})$ and $\lambda(c) = \lambda_c(\sqrt{\epsilon})$ have unique solutions as

$$c_H(\sqrt{\epsilon}) = \frac{u_m^2+k_2}{v_m} + \frac{u_m^2+k_1}{v_m(1-3u_m)}\epsilon + O\left(\epsilon^{\frac{3}{2}}\right) \tag{2.11}$$

and

$$\begin{aligned} c_c(\sqrt{\epsilon}) &= \frac{u_m^2+k_2}{v_m} + \frac{u_m^2+k_1}{v_m(1-3u_m)}\left[1-\frac{\hat{A}}{2\left(u_m^2+k_2\right)^2(1-3u_m)^2}\right]\epsilon \\ &\quad + O\left(\epsilon^{\frac{3}{2}}\right). \end{aligned} \tag{2.12}$$

3. Multi-scale dynamics

In this section, we mainly study the multi-scale dynamics of system (1.3). It is clear that the critical manifold M_0^2 is S-shape with two non-normally hyperbolic points $Q_m(u_m, v_m)$ and $Q_M(u_M, v_M)$. Based on Theorem 2.1, we classify the multi-scale dynamics of system (1.3) into three cases.

3.1. Single positive equilibrium

In this case, parameters $\eta = (c, k_1, k_2) \in D_1$. Choosing different values of parameters $\eta = (c, k_1, k_2)$, we will consider five different scenarios. See Fig.2. Note that the analysis methods and results of Cases (d) and (e) are similar to that of Cases (a) and (b). Hence, Cases (d) and (e) are ignored in this paper.

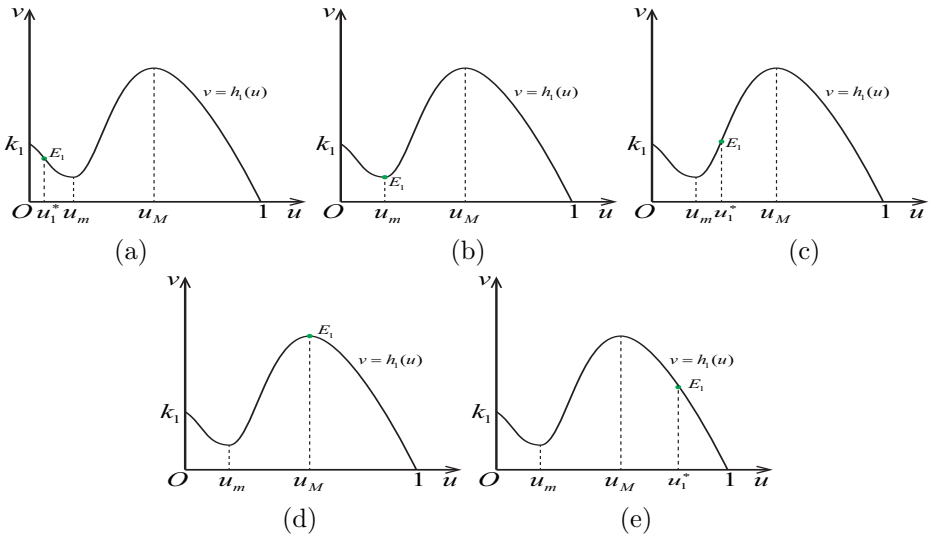

Figure 2. The different cases for the positive equilibrium's location, where (a) $0 < u_1^* < u_m$, (b) $u_1^* = u_m$, (c) $u_m < u_1^* < u_M$, (d) $u_1^* = u_M$ and (e) $u_M < u_1^* < 1$.

3.1.1. Case (a): $0 < u_1^* < u_m$

It is easy to see that the dynamics of degenerate system (2.1) and layer system (2.2) are shown in Fig.3(a). Hence, according to the Fenichel theorem, we have the following theorem about the equilibrium $E_1(u_1^*, v_1^*)$.

Theorem 3.1. *If parameters $\eta = (c, k_1, k_2) \in D_1$ and system (1.3) has a unique stable positive equilibrium $E_1(u_1^*, v_1^*) \in M_0^{2l}$. See Fig.5(a).*

3.1.2. Case (b): $u_1^* = u_m$

In this case, the point (u_m, v_m) is a canard point and the dynamics of degenerate system (2.1) and layer system (2.2) are given in Fig.3(b). It is clear that the trajectories of degenerate system (2.1) starting on the normally hyperbolic attracting

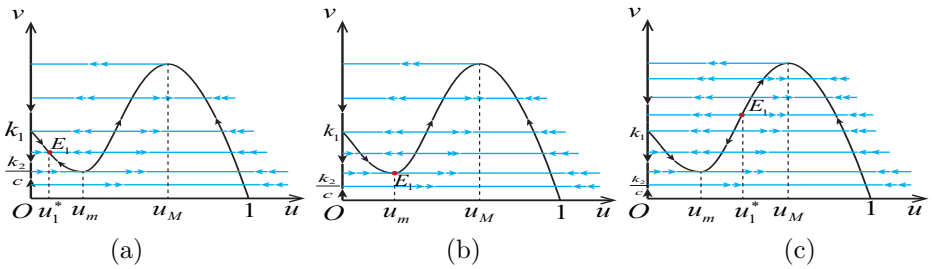

Figure 3. The dynamics of degenerate system (2.1) and layer system (2.2) when system (1.3) has one positive equilibrium satisfying (*a*) $0 < u_1^* < u_m$, (*b*) $u_1^* = u_m$ and (*c*) $u_m < u_1^* < u_M$.

critical manifold M_0^{2l} will pass through the canard point (u_m, v_m) and reach the normally hyperbolic repelling critical manifold M_0^{2m}. These trajectories may be perturbed to canard trajectories when $0 < \epsilon \ll 1$.

Before giving the main theorem about the canard cycles and relaxation oscillation cycle, we define a family of singular slow-fast cycles $\Gamma_0(s)$ for $s \in [0, s_0]$ where $s_0 = v_M - v_m$. Let $u^l(s)$, $u^m(s)$ and $u^r(s)$ be three positive roots of equation $h_1(u) = v_m + s$, which satisfy $u^l(s) < u^m(s) < u^r(s)$.

1. $\Gamma_0(0)$ is the canard point (u_m, v_m) and $\Gamma_0(s_0)$ is the singular slow-fast cycle corresponding to the relaxation oscillation cycle. See Fig.4(*c*).
2. For $s \in (0, k_1 - v_m]$, $\Gamma_0(s)$ is the singular slow-fast cycle corresponding to the canard cycle without head. See Fig.4(*a*), which has the following representation

$$\begin{aligned}\Gamma_0(s) = &\left\{(u,v) \mid v = h_1(u),\ u^l(s) < u < u^m(s)\right\} \\ &\cup \left\{(u,v) \mid v = s,\ u^l(s) \le u \le u^m(s)\right\}, \quad s \in (0, k_1 - v_m].\end{aligned}$$

3. For $s \in (k_1 - v_m, s_0)$, $\Gamma_0(s)$ is the singular slow-fast cycle corresponding to the canard cycle with head. See Fig.4(*b*), whose representation is

$$\begin{aligned}\Gamma_0(s) = &\{(u,v) \mid v = s,\ 0 \le u \le u^m(s)\} \cup \{(u,v) \mid u = 0,\ \hat{v}_* \le v \le s\} \\ &\cup \{(u,v) \mid v = \hat{v}_*,\ 0 < u < \hat{u}_*\} \\ &\cup \{(u,v) \mid v = h_1(u),\ \hat{u}_* < u < u^m(s)\}, \quad s \in (k_1 - v_m, s_0),\end{aligned}$$

where $\hat{v}_*$ is determined by Lemma 2.1 and $\hat{u}_*$ is the smallest solution of equation $h_1(u) = \hat{v}_*$.

The following theorem gives the existence of canard explosion phenomenon of system (1.3).

Theorem 3.2. *Suppose $\eta = (c, k_1, k_2) \in D_1$, the extreme point (u_m, v_m) is the canard point of system* (1.3) *and parameters c and λ satisfy the relationship* (2.7)*, then the following results of system* (1.3) *hold.*

1. *There exists c_0 such that for $\left|c - \frac{u_m^2 + k_2}{v_m}\right| < c_0$, system* (1.3) *has precisely one positive equilibrium $E_1(u_1^*, v_1^*)$ in the neighborhood of (u_m, v_m), which converges to (u_m, v_m) as $(c, \epsilon) \to (\frac{u_m^2 + k_2}{v_m}, 0)$, and it is stable with $c < c_H(\sqrt{\epsilon})$*

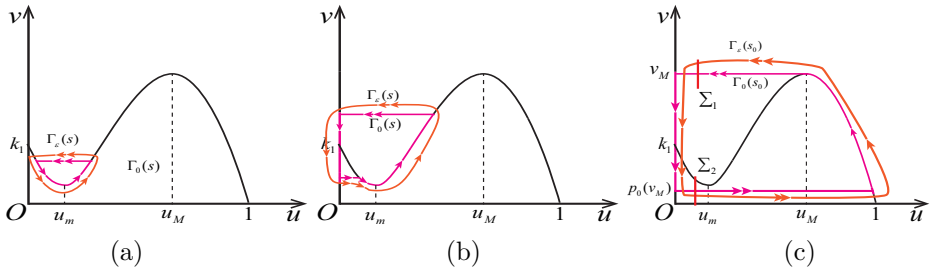

Figure 4. The singular slow-fast cycles, which correspond to the canard cycles and relaxation oscillation cycle.

given by (2.11) *and unstable with* $c > c_H(\sqrt{\epsilon})$. *Hence, there is a singular Hopf bifurcation when* c *passes through curve* $c_H(\sqrt{\epsilon})$. *Furthermore, the Hopf bifurcation is supercritical if* $\hat{A} < 0$ *and subcritical if* $\hat{A} > 0$.

2. *For* $s \in [0, s_0]$, *there exists a family of canard cycles parameterized by* $s \mapsto (c(s, \sqrt{\epsilon}), \Gamma_\epsilon(s))$, *which is bifurcated from the singular slow-fast cycle* $\Gamma_0(s)$, *and* $\Gamma_\epsilon(s) \to \Gamma_0(s)$ *as* $\epsilon \to 0$. *Moreover, the canard explosion occurs if* $s \in [\epsilon^\nu, 2s_0 - \epsilon^\nu]$, $\nu \in (0,1)$, *and there is a curve* $c = c_c(\sqrt{\epsilon})$ *given by* (2.12) *such that*
$$\left|c(s, \sqrt{\epsilon}) - c_c(\sqrt{\epsilon})\right| \le \exp(-1/\epsilon^\nu), \quad s \in [\epsilon^\nu, 2s_0 - \epsilon^\nu].$$

3. *Let* $v^0 = v_M$ *in* (2.5), *if* $I(v_m) < 0$, *then, when the canard cycle of system* (1.3) *occurs, the relaxation oscillation cycle and the canard cycle co-exist. Moreover, the relaxation oscillation cycle is stable and converges to the singular slow-fast cycle* $\Gamma(s_0)$ *in Hausdorff distance when* $\epsilon \to 0$.

Proof. Set that η_0 is the value parameters $\eta = (c, k_1, k_2)$ satisfying $v_m = \frac{u_m^2 + k_2}{c}$. A simple calculation shows that

$$\begin{aligned}
&f(u_m, v_m, \eta_0) = 0, \quad \frac{\partial f}{\partial u}(u_m, v_m, \eta_0) = 0, \quad g(u_m, v_m, \eta_0) = 0\\
&\frac{\partial^2 f}{\partial u^2}(u_m, v_m, \eta_0) = 2u_m(1 - 3u_m)\left(u_m^2 + k_2\right) > 0,\\
&\frac{\partial f}{\partial v}(u_m, v_m, \eta_0) = -u_m\left(u_m^2 + k_2\right) < 0,\\
&\frac{\partial g}{\partial u}(u_m, v_m, \eta_0) = 2v_m u_m\left(u_m^2 + k_1\right) > 0,\\
&\frac{\partial g}{\partial c}(u_m, v_m, \eta_0) = -u_m v_m\left(u_m^2 + k_1\right) < 0,
\end{aligned}$$

which imply that the extreme point (u_m, v_m) is a non-degenerate canard point. Since system (2.8) is the slow-fast normal form of system (1.3) in the neighborhood of canard point (u_m, v_m), then system (2.8) has the non-degenerate canard point $(0, 0)$.

According to Theorem 3.1 in [8], there exist ϵ_0 and λ_0 such that the system has an equilibrium p_e near $(0, 0)$ and $p_e \mapsto (0, 0)$ as $(\epsilon, \lambda) \to (0, 0)$. Furthermore, the singular Hopf bifurcation curve is $\lambda = \lambda_H(\sqrt{\epsilon})$ given by (2.9) such that p_e is stable for $\lambda < \lambda_H(\sqrt{\epsilon})$ and unstable for $\lambda > \lambda_H(\sqrt{\epsilon})$. Moreover, the Hopf bifurcation is

supercritical if $\hat{A} < 0$ and subcritical if $\hat{A} > 0$. Since $\lambda'(c) > 0$ and $\lambda(c) = \lambda_H(\sqrt{\epsilon})$ has a unique solution $c = c_H(\sqrt{\epsilon})$, then $\lambda < \lambda_H(\sqrt{\epsilon})$ is equal to $c < c_H(\sqrt{\epsilon})$. Hence, statement 1 is true.

For statement 2, according to Theorems 3.3 and 3.5 in [8] about the canard explosion, the similar analysis shows that it holds for system (1.3).

For statement 3, to begin with, we show that $p_0(v_M) < v_m$, which means the trajectories starting near (u_M, v_M) cannot arrive at the neighborhood of normally hyperbolic critical manifold M_0^{2l}. Clearly, we have $I(p_0(v_M)) = 0$ and $I(\hat{v})$ is a decreasing function because of Lemma 2.1. Since $I(v_m) < 0$ which implies $p_0(v_M) < v_m$, we can construct the singular slow-fast cycle $\Gamma_0(s_0)$. See Fig.4(c).

In what follows, we will give the existence and stability of the relaxation oscillation cycle and the idea is inspried by Theorem 3.2 in [24]. Firstly, we set two vertical sections, see Fig.4(c), as

$$\Sigma_1 = \{(u, v) \mid u = u_0, v \in I_1\} \quad \text{and} \quad \Sigma_2 = \{(u, v) \mid u = u_0, v \in I_2\},$$

where $0 < u_0 < u_m$, I_1 and I_2 are small closed segments whose centers are v_M and $p_0(v_M)$. Note that Σ_i, $i = 1, 2$ are transversal to the singular slow-fast cycle $\Gamma_0(s_0)$. Furthermore, we define the transition map $\Pi : \Sigma_1 \to \Sigma_1$ along the flow of (1.3), which consists of two parts

$$\Pi_1 : \Sigma_1 \to \Sigma_2 \quad \text{and} \quad \Pi_2 : \Sigma_2 \to \Sigma_1.$$

Next, we will analyse the properties of transition maps Π_i, $i = 1, 2$.

For $\Pi_1 : \Sigma_1 \to \Sigma_2$, based on Lemma 2.1, the trajectory of system (1.3) starting at a point $(u_0, v_0) \in \Sigma_1$ must cross the vertical section at point $(u_0, p_\epsilon(v_0)) \in \Sigma_2$, where $\lim_{\epsilon \to 0} p_\epsilon(v_0) = p_0(v_0)$. So we have $\Pi_1(u_0, v_0) = (u_0, p_\epsilon(v_0))$.

For $\Pi_2 : \Sigma_2 \to \Sigma_1$, since (u_M, v_M) is a generic fold point of system (1.3), then $\Pi_2 : \Sigma_2 \to \Sigma_1$ is also a contract map with the exponential rate $O(\mathrm{e}^{-1/\epsilon})$ because of Theorem 2.1 in [7].

Thus, the transition map $\Pi = \Pi_2 \circ \Pi_1$ is a contract map with the exponential rate $O(\mathrm{e}^{-1/\epsilon})$. According to the Contraction Mapping Theorem, there is a unique fixed point in Σ_1, which corresponds to the unique relaxation oscillation cycle $\Gamma_\epsilon(s_0)$. Furthermore, this relaxation oscillation cycle is a stable limiting cycle and converges to the singular slow-fast cycle $\Gamma_0(s_0)$ in the Hausdorff distance when $\epsilon \to 0$.

□

Example 3.1. Set $\epsilon = 0.001$, $k_1 = 0.2$ and $k_2 = 0.15$. It is clear that $c_c(\sqrt{\epsilon}) = 0.8669$ and Fig.5(b)-(e) show the canard explosion phenomenon, where (a) $c = 0.875$, (b) $c = 0.87$, (c) $c = 0.86$ and (d) $c = 0.85$. From Fig.5(b)-(e), we can see that the canard cycle is surrounded by the relaxation oscillation cycle.

3.1.3. Case (c): $u_m < u_1^* < u_M$

The single positive equilibrium $E_1(u_1^*, v_1^*)$ is on the normally hyperbolic repelling critical manifold M_0^{2m} and the dynamics of degenerate system (2.1) and layer system (2.2) are given in Fig.3(c). Clearly, $E_1(u_1^*, v_1^*)$ is an unstable node of system (1.3) and (u_m, v_m) and (u_M, v_M) are generic fold points. According to the Finichel's theorem and Theorem 2.1 in [7], the slow manifold M_ϵ^{2r} near M_0^{2r} jumps to the vicinity of another attracting critical manifold M_0^{1s} when it reaches the neighbourhood

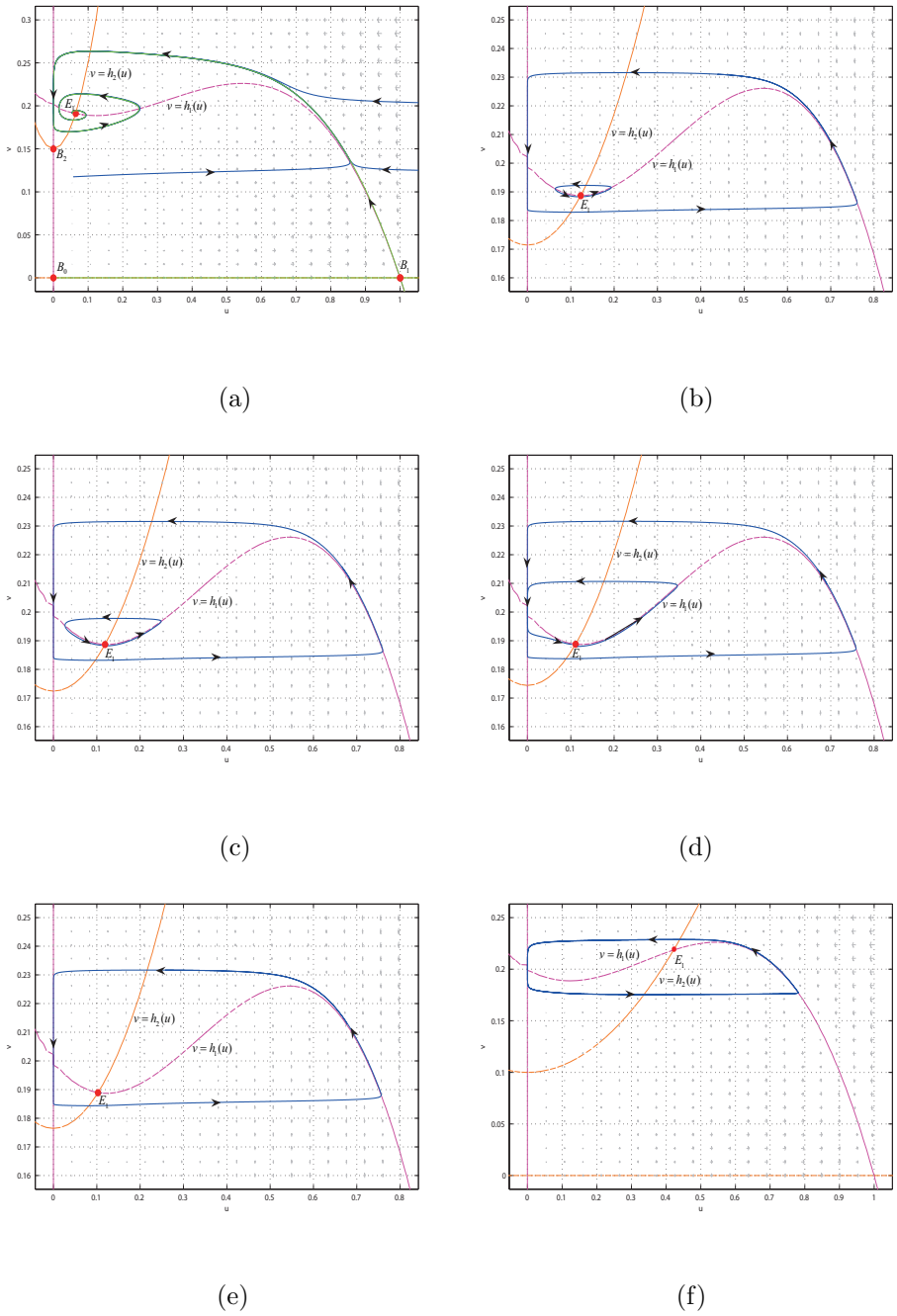

Figure 5. The phase portraits of system (1.3) with different values of parameters in the parameter region D.

of (u_M, v_M). Furthermore, using the entry-exit function theory, the similar result holds for the slow manifold M_ϵ^{1s} when it crosses the point $(0, k_1)$. Hence, using the similar analysis method of statement 3 in Theorem 3.2, we have the following theorem.

Theorem 3.3. *Suppose that parameters $\eta = (k_1, k_2, c) \in D_1$ and the single positive equilibrium $E_1(u_1^*, v_1^*) \in M_0^{2m}$. Then for $0 < \epsilon \ll 1$, there is a unique stable relaxation oscillation cycle $\Gamma_\epsilon(s_0)$, which converges to $\Gamma_0(s_0)$ in the Hausdorff distance with $\epsilon \to 0$.*

Example 3.2. Set $\epsilon = 0.001$, $k_1 = 0.2$, $k_2 = 0.15$ and $c = 1.5$ in (1.3). It is clear that there is a positive equilibrium $E_1(0.42158, 0.21849)$. Clearly, system (1.3) has a relaxation oscillation cycle. See Fig.5(f).

3.2. Two positive equilibriums

In this case, we have $\eta = (c, k_1, k_2) \in D_2^1 \cup D_2^2 \cup D_2^3$. Furthermore, system (1.3) has two positive equilibriums $E_1(u_1^*, v_1^*)$ and $E_2(u_2^*, v_2^*)$ whose locations have five different scenarios. See Fig.6.

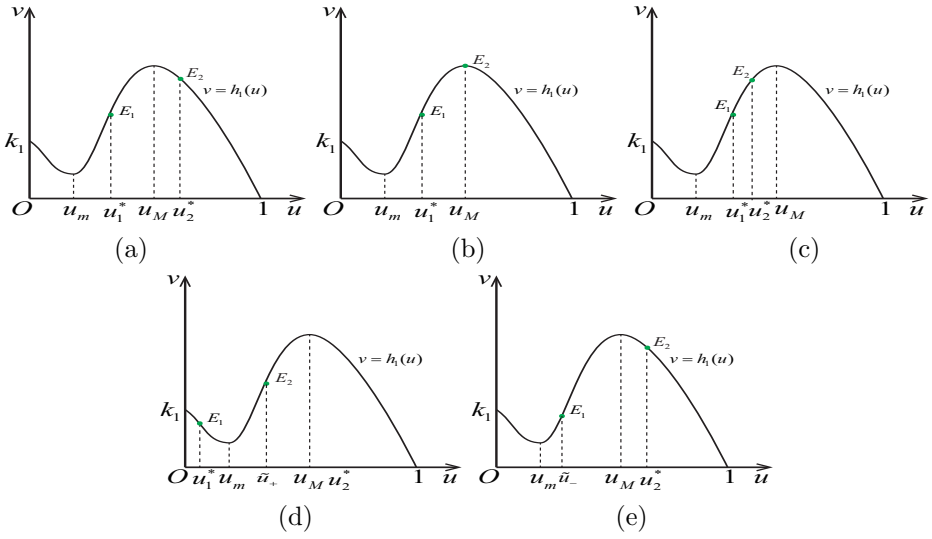

Figure 6. The different cases for the two positive equilibriums' location, where (*a*) $u_m < u_1^* < u_M < u_2^*$; (*b*) $u_m < u_1^* < u_M = u_2^*$; (*c*) $u_m < u_1^* < u_2^* < u_M$; (*d*) $u_1^* < u_m < u_2^* = \tilde{u}_+ < u_M$; (*e*) $u_m < u_1^* = \tilde{u}_- < u_M < u_2^*$.

3.2.1. Case (*a*): $u_m < u_1^* < u_M < u_2^*$

Now the positive equilibriums $E_1(u_1^*, v_1^*)$ and $E_2(u_2^*, v_2^*)$ respectively lie in the normally hyperbolic repelling critical submanifold M_0^{2m} and normally hyperbolic attracting critical submanifold M_0^{2r} and the dynamics of degenerate system (2.1) and layer system (2.2) are shown in Fig.7(*a*). Hence, according to the Finichel theorem, it is obvious that the equilibrium $E_1(u_1^*, v_1^*)$ is a saddle point and the equilibrium $E_2(u_2^*, v_2^*)$ is a stable node for $0 < \epsilon \ll 1$.

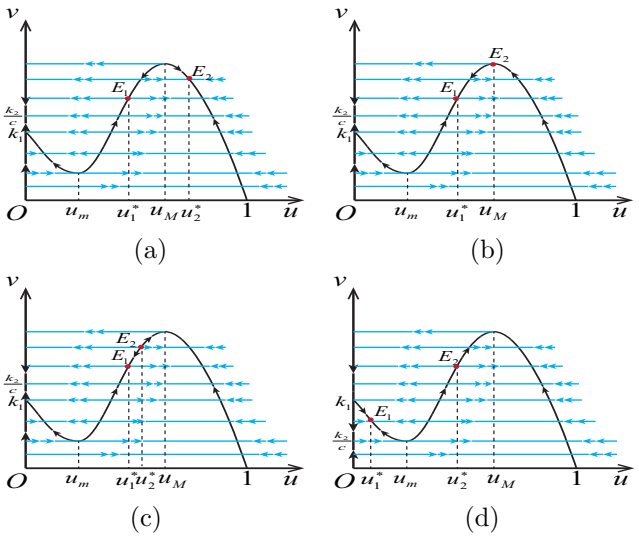

Figure 7. The dynamics of degenerate system (2.1) and layer system (2.2) when system (1.3) has two positive equilibriums satisfying (*a*) $u_m < u_1^* < u_M < u_2^*$, (*b*) $u_m < u_1^* < u_M = u_2^*$, (*c*) $u_m < u_1^* < u_2^* < u_M$ and (*d*) $u_1^* < u_m < u_2^* = \tilde{u}_+ < u_M$.

Theorem 3.4. *Suppose* $\eta = (c, k_1, k_2) \in D_2^1$ *and* $u_m < u_1^* < u_M < u_2^*$. *Then system* (1.3) *has a heteroclinic orbit from* $E_1(u_1^*, v_1^*)$ *to* $E_2(u_2^*, v_2^*)$ *and a heteroclinic orbit from* $E_1(u_1^*, v_1^*)$ *to* $B_2(0, \frac{k_2}{c})$.

Proof. Since $E_2(u_2^*, v_2^*)$ is a stable equilibrium of the degenerate system (2.1) and $W_0^u(E_1) \cap W_0^s(M_0^{2r}) \neq \oslash$, then there is a singular orbit connecting equilibriums $E_1(u_1^*, v_1^*)$ and $E_2(u_2^*, v_2^*)$. Moreover, $W_0^u(E_1) \cap W_0^s(M_0^{2r})$ is transverse by dimension counting. Since $W_0^u(E_1)$ perturbs to the unstable manifold $W_\epsilon^u(E_1)$ of saddle $E_1(u_1^*, v_1^*)$ and $W^s(M_0^{2r})$ perturbs to the two dimensional stable manifold $W_\epsilon^s(E_2)$ of equilibrium $E_2(u_2^*, v_2^*)$ based on the Finichel theorem, then $W_0^u(E_1) \cap W_\epsilon^s(E_2) \neq \oslash$ because of the transversality of $W_0^u(E_1) \cap W_0^s(M_0^{2r})$, which implies there is a heteroclinic orbit from $E_1(u_1^*, v_1^*)$ to $E_2(u_2^*, v_2^*)$.

With the similar analysis, we can prove there is a heteroclinic from $E_1(u_1^*, v_1^*)$ to $B_2(0, \frac{k_2}{c})$. Hence, the proof is complete.

□

Example 3.3. Set $\epsilon = 0.01$, $k_1 = 0.15$, $k_2 = 1.25$ and $c = 8$ in (1.3), it is clear that there are two positive equilibriums $E_1(0.29524, 0.16715)$ and $E_2(0.61422, 0.20341)$ and the boundary equilibrium $B_2(0, 0.15625)$. Clearly, system (1.3) has two heteroclinic orbits. See Fig.8 (*a*).

3.2.2. Case (*b*): $u_m < u_1^* < u_M = u_2^*$

In this case, the extreme point (u_M, v_M) is a canard point of system (1.3) and the dynamics of degenerate system (2.1) and layer system (2.2) are shown in Fig.7(*b*). Similarly, the equilibrium $E_1(u_1^*, v_1^*)$ is a saddle point and the following theorem holds.

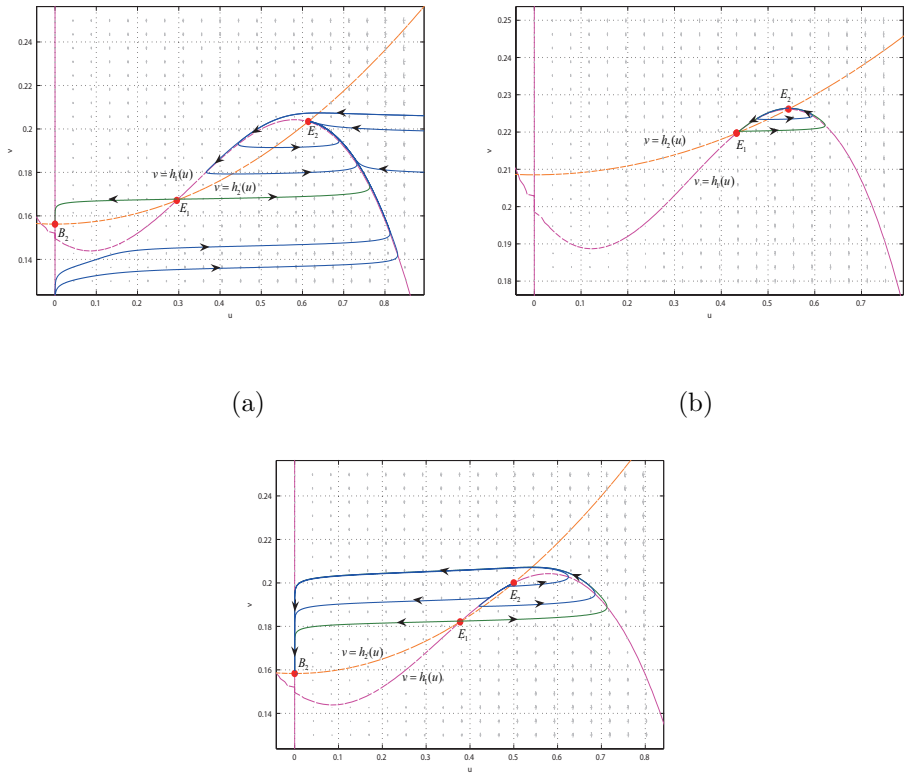

(a) (b)

(c)

Figure 8. The phase portraits of system (1.3) when it has two equilibriums satisfying (a) $u_m < u_1^* < u_M < u_2^*$; (b) $u_m < u_1^* < u_M = u_2^*$; (c) $u_m < u_1^* < u_2^* < u_M$.

Theorem 3.5. *Suppose that* $\eta = (c, k_1, k_2) \in D_2^1$, $u_m < u_1^* < u_M = u_2^*$ *and the extreme point* (u_M, v_M) *is a canard point. Then the following conclusions hold.*

1. *For* $s \in (0, v_M - v_1^*)$, *system* (1.3) *has a family of canard cycles without head parameterized by* $s \mapsto (c(s, \sqrt{\epsilon}), \Gamma_\epsilon(s))$, *which emerge from the singular slow-fast cycles* $\Gamma_0(s)$, *and* $\Gamma_\epsilon(s) \to \Gamma_0(s)$ *as* $\epsilon \to 0$;
2. *System* (1.3) *has a unique homoclinic orbit of the saddle* $E_1(u_1^*, v_1^*)$ *if and only if* $c = \tilde{c}_c(\sqrt{\epsilon})$, *which is obtained by using* (u_M, v_M) *instead of* (u_m, v_m) *in* (2.12).

Proof. The proof conclusion 1 is omitted because it is similar to that of Theorem 3.2. Next, we give the proof conclusion 2. According to the Finichel theorem and the structure of $E_1(u_1^*, v_1^*)$, the stable manifold of $E_1(u_1^*, v_1^*)$ must be one of the slow manifolds, which is denoted as M^{2m}_{ϵ,E_1}. See Fig.9. Furthermore, the unstable manifold of $E_1(u_1^*, v_1^*)$ must be attracted to the $O(\epsilon)$ neighborhood of M_0^{2r} and move positively along M_0^{2r}. Finally, it will become a slow manifold emerged from M_0^{2r}, which is denoted as M^{2r}_{ϵ,E_1}. See Fig.9. In what follows, we will analyse the connecting condition of M^{2m}_{ϵ,E_1} and M^{2r}_{ϵ,E_1}.

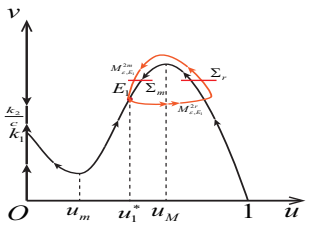

Figure 9. The homoclinic orbit of system (1.3) in equilibrium $E_1(u_1^*, v_1^*)$.

Set $\Sigma_i = \{(u, v_M - \rho^2) \mid u \in I_i\}$, $i = m, r$, see Fig.9, where ρ is a small parameter and I_i, $i = m, r$ are suitable regions. Furthermore, $q_{i,\epsilon}$, $i = m, r$ are the intersecting points between I_i and M^{2i}_{ϵ,E_1}. We define the transition map $\pi : \Sigma_r \to \Sigma_m$. Based on the Theorem 3.2 in [7], it is clear that $\pi(q_{r,\epsilon}) = q_{m,\epsilon}$ is equal to the existence of a continuous function $c = \tilde{c}_c(\sqrt{\epsilon})$ which is obtained by using (u_M, v_M) instead of (u_m, v_m) in (2.12). This implies that the stable manifold and unstable manifold of $E_1(u_1^*, v_1^*)$ intersect, which is the homoclinic orbit of system (1.3) in $E_1(u_1^*, v_1^*)$. Moreover, the equilibrium $E_2(u_2^*, v_2^*)$ is located in the region surrounded by this homoclinic orbit.

□

Example 3.4. Set $\epsilon = 0.005$, $k_1 = 0.2$, $k_2 = 3.5$ in (1.3). It is clear that there are two positive equilibriums $E_1(0.43283, 0.21969)$ and $E_2(0.54382, 0.22615)$ and the value of maximal canard curve $\tilde{c}_c(\sqrt{\epsilon}) = 16.7844$. Form Fig.8 (b), system (1.3) has a homoclinic orbit of equilibrium E_1.

3.2.3. Case (c): $u_m < u_1^* < u_2^* < u_M$

In this case, the dynamics of degenerate system (2.1) and layer system (2.2) are shown in Fig.7(c). Clearly, $E_1(u_1^*, v_1^*)$ is a saddle and $E_2(u_2^*, v_2^*)$ is an unstable node. Furthermore, the following theorem holds with the similar analysis of Theorem 3.4.

Theorem 3.6. *Suppose* $\eta = (c, k_1, k_2) \in D_2^1$ *and* $u_m < u_1^* < u_2^* < u_M$. *Then system* (1.3) *has two heteroclinic orbits from* $E_1(u_1^*, v_1^*)$ *to* $B_2(0, \frac{k_2}{c})$ *and infinite heteroclinic orbits from* $E_2(u_2^*, v_2^*)$ *to* $B_2(0, \frac{k_2}{c})$.

Example 3.5. Set $\epsilon = 0.01$, $k_1 = 0.15$, $k_2 = 0.95$ and $c = 6$ in (1.3). It is clear that there are two positive equilibriums $E_1(0.37749, 0.18208)$ and $E_2(0.5, 0.2)$ and a boundary equilibrium $B_2(0, 0.15833)$. Form Fig.8(c), there are two heteroclinic orbits connecting equilibriums E_1 and B_2 and infinite heteroclinic orbits connecting equilibriums E_2 and B_2.

3.2.4. Case (d): $u_1^* < u_m < u_2^* = \tilde{u}_+ < u_M$

In this case, the dynamics of degenerated system (2.1) and layer system (2.2) are shown in Fig.7(d). Clearly, $E_1(u_1^*, v_1^*)$ is a stable node and $E_2(u_2^*, v_2^*)$ is a saddle-node. According to the Theorem 5.6 in [23], the following theorem holds.

Theorem 3.7. *Suppose* $\eta = (c, k_1, k_2) \in D_2^3$ *and* $u_1^* < u_m < u_2^* < u_M$. *Then the equilibrium* $E_1(u_1^*, v_1^*)$ *is an attractor in the first quadrant and the flows tend to* $E_1(u_1^*, v_1^*)$ *except the stable manifold of* $E_2(u_2^*, v_2^*)$.

Remark 3.1. The analysis of case (e) is omitted because its conclusion and method are similar to those of case (d).

3.3. Three positive equilibriums

In this case, we have $\eta = (c, k_1, k_2) \in D_3^1$ and system (1.3) has three equilibriums $E_1(u_1^*, v_1^*)$, $E_2(u_2^*, v_2^*)$ and $E_3(u_3^*, v_3^*)$ whose locations have eight scenarios, see Fig.10. Note that the analysis of cases $(f)-(h)$ is omitted because their conclusions and methods are similar to those of cases (b), (c) and (e).

3.3.1. Case (a): $u_1^* < u_m < u_2^* < u_M < u_3^*$

The dynamics of degenerate system (2.1) and layer system (2.2) are shown in Fig.11(a). Furthermore, using the Finichel theorem, $E_1(u_1^*, v_1^*)$ and $E_3(u_3^*, v_3^*)$ are stable nodes and $E_2(u_2^*, v_2^*)$ is a saddle point. We have the following theorem by the similar analysis of Theorem 3.4.

Theorem 3.8. *Suppose* $\eta = (c, k_1, k_2) \in D_3^1$ *and* $u_1^* < u_m < u_2^* < u_M < u_3^*$. *Then system* (1.3) *has a heteroclinic orbit from* $E_2(u_2^*, v_2^*)$ *to* $E_1(u_1^*, v_1^*)$ *and a heteroclinic orbit from* $E_2(u_2^*, v_2^*)$ *to* $E_3(u_3^*, v_3^*)$.

Example 3.6. Set $\epsilon = 0.01$, $k_1 = 0.2$, $k_2 = 1.9$ and $c = 10$ in (1.3). It is clear that there are three positive equilibriums $E_1(0.01016, 0.1905)$, $E_2(0.23973, 0.19575)$ and $E_3(0.258951, 0.22475)$ and two heteroclinic orbits. See Fig.12 (a).

3.3.2. Case (b): $u_1^* = u_m < u_2^* < u_M < u_3^*$

In this case, the dynamics of degenerate system (2.1) and layer system (2.2) are shown in Fig.11(b). Clearly, (u_m, v_m) is a canard point, $E_3(u_3^*, v_3^*)$ is a stable node and $E_2(u_2^*, v_2^*)$ is a saddle point. Furthermore, we have the following theorem with the similar analysis in Theorems 3.4 and 3.5.

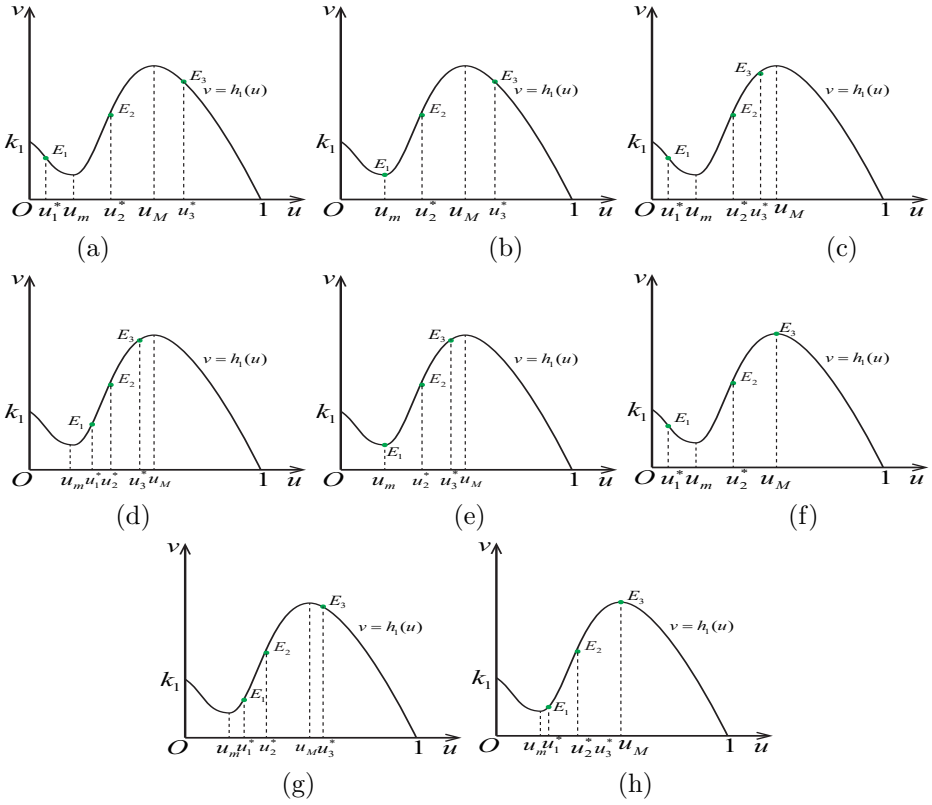

Figure 10. Eight different cases when system (1.3) has three positive equilibriums.

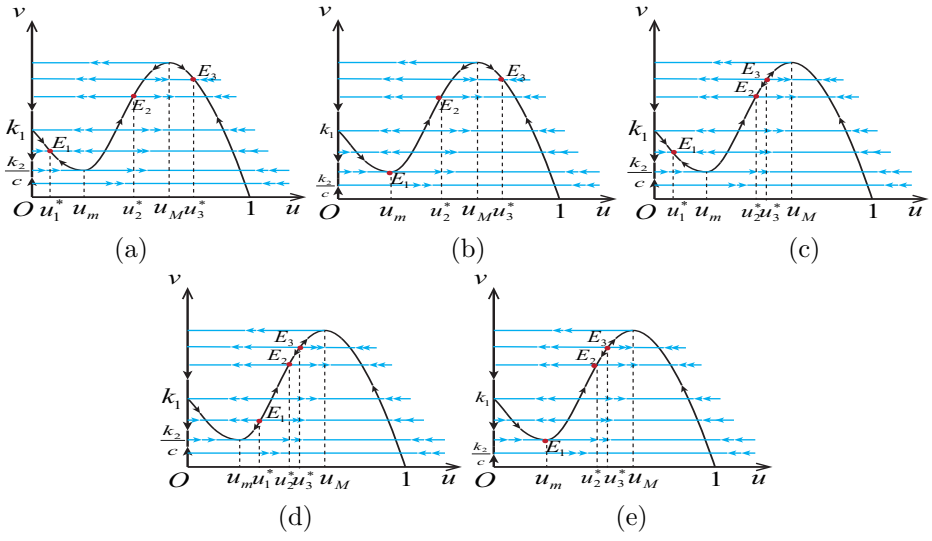

Figure 11. The dynamics of degenerate system (2.1) and layer system (2.2) when system (1.3) has three positive equilibriums satisfying (*a*) $u_1^* < u_m < u_2^* < u_M < u_3^*$; (*b*) $u_1^* = u_m < u_2^* < u_M < u_3^*$; (*c*) $u_1^* < u_m < u_2^* < u_3^* < u_M$; (*d*) $u_m < u_1^* < u_2^* < u_M < u_3^*$; (*e*)$u_1^* = u_m < u_2^* < u_3^* < u_M$.

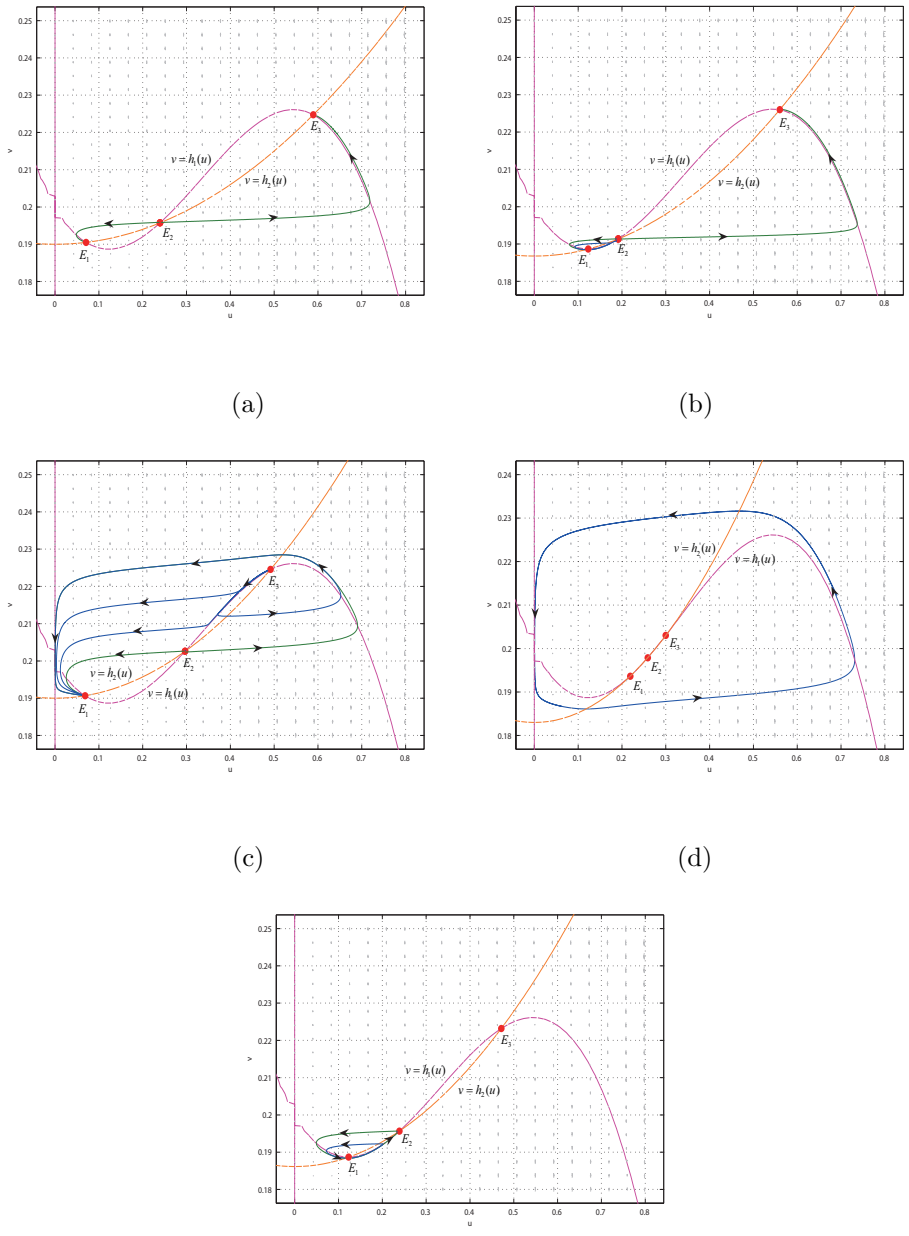

Figure 12. The phase portraits of system (1.3) when it has three positive equilibriums satisfying (a) $u_1^* < u_m < u_2^* < u_M < u_3^*$; (b) $u_1^* = u_m < u_2^* < u_M < u_3^*$; (c) $u_1^* < u_m < u_2^* < u_3^* < u_M$; (d) $u_m < u_1^* < u_2^* < u_M < u_3^*$; (e) $u_1^* = u_m < u_2^* < u_3^* < u_M$.

Theorem 3.9. *Suppose $\eta = (c, k_1, k_2) \in D_3^1$, $u_1^* = u_m < u_2^* < u_M < u_3^*$ and the extreme point (u_m, v_m) is a canard point. Then the following conclusions hold.*

1. *For $s \in (0, v_2^* - v_m)$, system (1.3) has a family of canard cycles without head parameterized by $s \mapsto (c(s, \sqrt{\epsilon}), \Gamma_\epsilon(s))$, which emerge from the singular slow-fast cycle $\Gamma_0(s)$, and $\Gamma_\epsilon(s) \to \Gamma_0(s)$ as $\epsilon \to 0$;*
2. *System (1.3) has a unique homoclinic orbit in the saddle $E_2(u_2^*, v_2^*)$ if and only if $c = c_c(\sqrt{\epsilon})$;*
3. *System (1.3) has a heteroclinic orbit from $E_2(u_2^*, v_2^*)$ to $E_3(u_3^*, v_3^*)$.*

Example 3.7. Set $\epsilon = 0.005$, $k_1 = 0.2$, $k_2 = 1.4943$ in (1.3). It is clear that there are three positive equilibriums $E_1(0.12328, 0.18867)$, $E_2(0.19161, 0.19136)$ and $E_3(0.56012, 0.22598)$ and the value of canard explosion curve $c_c(\sqrt{\epsilon}) = 8.0008$. Hence, from Fig.12($b$), we can see that there is a homoclinic orbit in E_2 and a heteroclinic orbit connecting equilibriums E_2 and E_3.

3.3.3. Case (c): $u_1^* < u_m < u_2^* < u_3^* < u_M$

In this case, the dynamics of the degenerate system (2.1) and the layer system (2.2) are shown in Fig.11(c). Clearly, $E_1(u_1^*, v_1^*)$ is a stable node, $E_3(u_3^*, v_3^*)$ is an unstable node and $E_2(u_2^*, v_2^*)$ is a saddle point. Furthermore, we have the following theorem with the similar analysis of Theorem 3.4.

Theorem 3.10. *Suppose $\eta = (c, k_1, k_2) \in D_3^1$ and $u_m < u_1^* < u_2^* < u_M < u_3^*$. Then system (1.3) has two heteroclinic orbits from $E_2(u_2^*, v_2^*)$ to $E_1(u_1^*, v_1^*)$ and infinite heteroclinic orbits from $E_3(u_3^*, v_3^*)$ to $E_1(u_1^*, v_1^*)$.*

Example 3.8. Set $\epsilon = 0.01$, $k_1 = 0.2$, $k_2 = 1.23$ and $c = 7$ in (1.3). It is clear that there are three positive equilibriums $E_1(0.068505, 0.19067)$, $E_2(0.29678, 0.20258)$ and $E_3(0.49185, 0.22456)$. From Fig.12(c), system (1.3) has two heteroclinic orbits connecting equilibriums E_2 and E_1 and infinite heteroclinic orbits connecting equilibriums E_3 and E_1.

3.3.4. Case (d): $u_m < u_1^* < u_2^* < u_3^* < u_M$

In this case, the dynamics of degenerate system (2.1) and layer system (2.2) are shown in Fig.11(d). Clearly, $E_1(u_1^*, v_1^*)$ and $E_3(u_3^*, v_3^*)$ are unstable nodes and $E_2(u_2^*, v_2^*)$ is a saddle point. Furthermore, it is easy to get the following theorem by using the similar method of Theorem 3.3.

Theorem 3.11. *Suppose $\eta = (c, k_1, k_2) \in D_3^1$ and $u_m < u_1^* < u_2^* < u_3^* < u_M$. Then there is a relaxation oscillation cycle of system (1.3) around three positive equilibriums.*

Example 3.9. Set $\epsilon = 0.01$, $k_1 = 0.2$, $k_2 = 0.8235$ and $c = 4.5$ in (1.3). It is clear that there are three positive equilibriums $E_1(0.21886, 0.19364)$, $E_2(0.25892, 0.1979)$ and $E_3(0.3, 0.203)$ and a relaxation oscillation cycle. See Fig.12(d).

3.3.5. Case (e): $u_1^* = u_m < u_2^* < u_3^* < u_M$

In this case, the dynamics of degenerate system (2.1) and layer system (2.2) are shown in Fig.11(e). Clearly, (u_m, v_m) is a canard point, $E_3(u_3^*, v_3^*)$ is an unstable

stable node and $E_2(u_2^*, v_2^*)$ is a saddle point. Furthermore, the following theorem holds with the similar analysis of Theorem 3.5.

Theorem 3.12. *Suppose $\eta = (c, k_1, k_2) \in D_3^1$, $u_1^* = u_m < u_2^* < u_3^* < u_M$ and the extreme point (u_M, v_M) is a canard point. Then the following conclusions hold.*

1. *For $s \in (0, v_2^* - v_m)$, system (1.3) has a family of canard cycles without head parameterized by $s \mapsto (c(s, \sqrt{\epsilon}), \Gamma_\epsilon(s))$, which emerge from the singular slow-fast cycle $\Gamma_0(s)$, and $\Gamma_\epsilon(s) \to \Gamma_0(s)$ as $\epsilon \to 0$;*
2. *There is a homoclinic orbit of system (1.3) in equilibrium $E_1(u_1^*, v_1^*)$ if and only if $c = c_c(\sqrt{\epsilon})$.*

Example 3.10. Set $\epsilon = 0.005$, $k_1 = 0.2$, $k_2 = 1.117$ in (1.3). It is clear that there are three positive equilibriums $E_1(0.12313, 0.18867)$, $E_2(0.23869, 0.19564)$ and $E_3(0.47154, 0.22319)$ and the value of canard explosion curve $c_c(\sqrt{\epsilon}) = 6.0008$. Hence, from Fig.12($e$), we can see that there is a homoclinic orbit of equilibrium E_2.

4. Discussion

In this paper, under the assumption that the growth rate of preys is much larger than that of predators, we introduce a small positive parameter into a Leslie-Gower prey-predator model with Monod-Haldane function response and yield a slow-fast system (1.3). We analyse the number and locations of positive equilibriums in system (1.3) and obtain rich dynamics such as canard phenomenon, relaxation oscillation cycle, heteroclinic and homoclinic orbits and so on. Especially, the relaxation oscillation cycle and canard cycle co-exist when system (1.3) only has one positive equilibrium $E_1(u_1^*, v_1^*)$ with $0 < u_1^* = u_m < u_M$. All these dynamics have practical biological significance and, as an example, we illustrate biological phenomenon of the canard cycle without head in Section 3.1.2. See Fig.5(b) and (c).

For Fig.5(b) and (c), the slow manifold stands for the density of predators and preys change very slowly while the fast orbits stand for the density of preys change dramatically. Therefore, the canard cycle suggests that the density of predators grow slow when the density of preys can support the reproduction of predators. However, once the density of predators is over the tolerance of preys, the density of preys decrease dramatically. This leads to a slow decrease in the density of predators because of the low density of preys and the density of preys recovers slowly until a new cycle starts.

Acknowledgements

The first author is supported by the Fundamental Research Funds for the Central Universities (No.2232023D-22), the Natural Science Foundation of Shanghai (No.24YF2700900) and the Donghua University 2024 Cultivation Project of Discipline Innovation. The second author is supported by the National Natural Science Foundation of China(No.12371168) the Science and Technology Commission of Shanghai Municipality (No.18dz2271000).

References

[1] B. Ambrosio, M. A. Aziz–Alaoui and R. Yafia, *Canard phenomenon in a slow-fast modified Leslie-Gower model*, Math. Biosci., 2018, 295, 48–54.

[2] A. Atabaigi and A. Barati, *Relaxation oscillations and canard explosion in a predator-prey system of Holling and Leslie types*, Nonlinear Anal. Real World Appl., 2017, 36, 139–153.

[3] H. Cai, A. Ghazaryan and V. Manukian, *Fisher-KPP dynamics in diffusive Rosenzweig-MacArthur and Holling-Tanner models*, Math. Model. Nat. Phenom., 2019, 14, 404–425.

[4] N. Finichel, *Geometric singular perturbation theory for ordinary differential equations*, J. Diff. Equ., 1979, 55, 763–783.

[5] A. Ghazaryan, V. Manukian and S. Schecter, *Travelling waves in the Holling-Tanner model with weak diffusion*, Proc. R. Soc. Lond. Ser. A, 2015, 471, 20150045.

[6] G. Hek, *Geometric singular perturbation theory in biological practice*, J. Math. Biol., 2010, 60, 347–386.

[7] M. Krupa and P. Szmolyan, *Extending geometric singular perturbation theory to nonhyperbolic points-fold and canard points in two dimensions*, SIAM J. Math. Anal., 2001, 33, 286–314.

[8] M. Krupa and P. Szmolyan, *Relaxation oscillation and canard explosion*, J. Diff. Equ., 2001, 174, 312–368.

[9] C. Kuehn, *Multiple Time Scale Dynamics*, 2015.

[10] C. Z. Li and H. P. Zhu, *Canard cycles for predator-prey systems with Holling types of functional response*, J. Diff. Equ., 2013, 254, 879–910.

[11] C. Z. Li, J. Q. Li, Z. E. Ma and H. P. Zhu, *Canard phenomenon for an SIS epidemic model with nonlinear incidence*, J. Math. Anal. Appl., 2014, 420, 987–1004.

[12] S. B. Li, J. H. Wu and H. Nie, *Steady-state bifurcation and Hopf bifurcation for a diffusive Leslie-Gower predator-prey model*, Comput. Math. Appl., 2015, 70, 3043–3056.

[13] W. S. Liu, *Exchange lemmas for singular perturbation problems with certain turning points*, J. Diff. Equ., 2000, 167, 134–180.

[14] W. S. Liu, *Geometric singular perturbations for multiple turning points: invariant manifolds and exchange lemmas*, J. Dyn. Differ. Equations, 2006, 18, 667–691.

[15] W. S. Liu, D. M. Xiao and Y. Yi, *Relaxation oscillations in a class of predator-prey systems*, J. Diff. Equ., 2003, 188, 306–331.

[16] P. De Maesschalck and S. Schecter, *The entry-exit function and geometric singular perturbation theory*, J. Diff. Equ., 2016, 260, 6697–6715.

[17] V. Manukian, *On traveling waves of Gray-Scott model*, Dyn. Syst. Int. J., 2015, 30, 270–296.

[18] E. Shchepakina, *Black swans and canards in two predator-one prey model*, Math. Model. Nat. Phenom., 2019, 14, 408–420.

[19] J. H. Shen, *Canard limit cycles and global dynamics in a singularly perturbed predator-prey system with non-monotonic functional response*, Nonlinear Anal. Real World Appl., 2016, 31, 146–165.

[20] J. H. Shen, C. H. Hsu and T. H. Yang, *Fast-slow dynamics for intraguild predation models with evolutionary effects*, J. Dyn. Differ. Equations, 2020, 32, 895–920.

[21] W. Sokol and J. A. Howell, *Kinetics of phenol oxidation by washed cells*, Biotechnol. Bioeng., 1981, 23, 2039–2049.

[22] C. Wang and X. Zhang, *Stability loss delay and smoothness of the return map in slow-fast systems*, SIAM J. Appl. Dyn. Syst., 2018, 17, 788–822.

[23] C. Wang and X. Zhang, Canards, *heteroclinic and homoclinic orbits for a slow-fast predator-prey model of generalized Holling type III*, J. Diff. Equ., 2019, 267, 3397–3441.

[24] C. Wang and X. Zhang, *Relaxation oscillations in a slow-fast modified Leslie-Gower model*, Appl. Math. Lett., 2019, 87, 147–153.

[25] Y. Q. Zhang, Y. C. Zhou and B. Tang, *Canard phenomenon in an SIRS epidemic model with nonlinear incidence rate*, Internat. J. Bifur. Chaos Appl. Sci. Engrg., 2020, 30, 2050073, 19 pp.

[26] R. Zou, S. J. Guo, *Dynamics of a diffusive Leslie-Gower predator-prey model in spatially heterogeneous environment*, Discrete Contin. Dyn. Syst., Ser. B, 2020, 25, 4189–4210.